Carbohydrate Polymers 102 (2014) 231–237

Contents lists available at ScienceDirect

Carbohydrate Polymers

journal homepage: www.elsevier.com/locate/carbpol

# Antibacterial activity of polyacrylonitrile–chitosan electrospun nanofibers

Sam Soo Kim [a], Jaewoong Lee [b,*]

[a] Department of Textile Engineering & Technology, Yeungnam University, Gyeongsan 712-749, South Korea
[b] Korean Intellectual Property Office, Daejeon 302-701, South Korea

ARTICLE INFO

*Article history:*
Received 26 October 2013
Received in revised form
20 November 2013
Accepted 21 November 2013
Available online 1 December 2013

*Keywords:*
Polyacrylonitrile
Chitosan
Nanofiber
Antibacterial

ABSTRACT

Polyacrylonitrile (PAN)–chitosan double-face films and nanofibers were manufactured. PAN and a chitosan salt were dissolved in dimethyl sulfoxide, and then thin-layered on a glass plate or electro-spun followed by coagulation in sodium hydroxide solution. The morphology of the PAN–chitosan double-face films and nanofibers was analyzed by scanning electron microscopy. The thermal behavior and the glass transition temperature of PAN–chitosan blends were assessed by differential scanning calorimetry and dynamic mechanical analysis, respectively. The antibacterial efficacy was measured by a swatch test with bacterial suspensions. The PAN–chitosan nanofibers produced a 5-log reduction against *Escherichia coli*, *Staphylococcus aureus*, and *Micrococcus luteus*.



## 1. Introduction

As consumers have concerned to sanitization of their belongings including cloth, research for an antibacterial fiber has been attracted (Dastjerdi & Montazer, 2010; Gao & Cranston, 2008). An antibacterial fiber has been produced using fiber forming polymers and antibacterial materials. Typically commercialized fiber polymers such as nylon, polyester, and acryl possess excellent fiber-forming ability. In addition to fiber-forming ability, such commercialized fibers could be altered into antibacterial fibers with antibacterial materials (Nataraj, Yang, & Aminabhavi, 2012; Ren et al., 2008, 2009; Shi, Vitchuli, Nowak, Caldwell, et al., 2011; Shi, Vitchuli, Nowak, Noar, et al., 2011). To produce antibacterial fibers, some antibacterial compounds have been suggested. For instance, quaternary ammonium compounds (Kim & Sun, 2001; Zhu & Sun, 2004), metal and metal salts (Jeong, Hwang, & Yi, 2005; Nakashima, Sakagami, & Matsuo, 2001), photocatalyst (Takahashi, Shoji, Inoue, Miyamoto, & Tokuda, 2004), *N*-halamines (Kim, Kim, Huang, Whang, & Lee, 2009; Lee & Whang, 2011), and chitosan (Chaudhari & Murthy, 2013; Torres-Giner, Ocio, & Lagaron, 2008) have been employed. Among those antibacterial compounds, chitosan, the cationic (1-4)-2-amino-2-deoxy-β-D-glucan, is industrially produced from marine chitin (Muzzarelli, 1993; Muzzarelli et al., 2012). Chitosan and its derivatives have a wide spectrum of biological activities, among which the bactericidal and bacteriostatic actions. Chitosan promotes the disorganization of the bacterial cell wall and cytoplasmic membrane, thus promoting the loss of cellular fluids, finally resulting either in bacterial death or inactivation, depending on the strains examined (Muzzarelli et al., 1990; Sudarshan, Hoover, & Knorr, 1992; Wan, Wu, Yu, & Wen, 2006).

Because chitosan dissolves easily in most acid solutions, some fiber-forming polymers such as nylon (Zhang et al., 2009), cellulose acetate (Liu & Bai, 2006), and polyvinyl alcohol (Srinivasa, Ramesh, Kumar, & Tharanathan, 2003) were blended with chitosan. Regarding blending with PAN, Nam, Kim, and Ko (1999) and Nam, Kim, and Ko (2001) reported PAN copolymer/chitosan salt blend produced by a wet-spinning process. However, the chitosan salt in the PAN copolymer/chitosan salt blend may possess risk of dissolving in water during conventional applications. Moreover, little research has been done on the nanofibrous PAN–chitosan blend and its antibacterial efficacy.

The aim of this study was to produce PAN–chitosan electrospunn nanofibers which were insoluble in water with relatively large surface area, and to measure the antibacterial activity of the electrospunn nanofibers. Our attention was particularly paid on antibacterial efficacy of PAN–chitosan films and nanofibers for better understanding antibacterial properties of chitosan in the blend.

* Corresponding author. Tel.: +82 42 481 8716; fax: +82 42 472 3558.
*E-mail address:* leejaew@hotmail.com (J. Lee).

0144-8617/$ – see front matter © 2013 Elsevier Ltd. All rights reserved.
http://dx.doi.org/10.1016/j.carbpol.2013.11.028

## 2. Experimental

### 2.1. Materials

PAN was purchased from Sigma-Aldrich (St. Louis, MO, USA). The weight-average molecular weight of the PAN was 150,000. Chitosan (viscosity 13–14 cps, degree of deacetylation was 95.4%) was obtained from YB Biochemical (Yeongdeok, Korea). Dimethyl sulfoxide (DMSO) and *N,N*-dimethylacetamide (DMAc) were purchased from Daejung Chemicals (Shiheung, Korea) and were used without further purification.

### 2.2. Preparation of PAN–chitosan double-face films

Chitosan (1.5 g) was dissolved in 100 mL of distilled water with methane sulfonic acid (1 g) at ambient temperature for 1 h and then freeze-dried (Freeze dryer, FDA5518, Ilshin Engineering, Siheung, Korea) at −70 °C for 48 h (Sashiwa, Shigemasa, & Roy, 2000). The ratio of PAN to chitosan was varied at 100/0, 95/5, 85/15, 75/25, 50/50, 25/75, and 0/100 wt%. The concentration of the solutions was fixed at 15 wt%. A homogeneous 15 wt% PAN/chitosan (50/50 wt%) solution was prepared by adding 7.5 g of PAN into 100 mL of DMSO, while stirring, at 65 °C for 4 h followed by cooling at 50 °C. Then, 7.5 g of freeze dried chitosan–methane sulfonic acid salt was added into the PAN solution with additional stirring for 4 h.

The film was produced through a film-making process using a Baker applicator (YBA-4, Yoshimitsu Seiki, Tokyo, Japan). The solution was thin-layered on a glass plate using the Baker applicator; the glass plate (200 mm × 300 mm × 5 mm) was then dipped into a 1% sodium hydroxide (NaOH) solution at ambient temperature for 6 h followed by dipping into distilled water at ambient temperature for 12 h and then at 80 °C for 10 min. The film was sandwiched using a non-woven fabric to minimize rolling up of the edge, and then the film was dried at ambient temperature for 24 h. The thickness of the films was measured by a dial thickness gauge (Peacock Dial Thickness Gauge H, Ozaki Mfg, Ozaki, Japan) after drying. The thickness of the film was approximately 100 μm. The films were used to determine the thermal properties and molecular interaction of the PAN–chitosan blend.

### 2.3. Preparation of PAN–chitosan electrospun nanofibers

DMSO/DMAc co-solvent system (50/50, v/v) was applied for electro-spinning. The PAN/chitosan solutions for electro-spinning were similar to those used for the preparation of films except that DMAc and DMSO were separately used for PAN and chitosan, respectively. For instance, a homogeneous 15 wt% PAN/chitosan (50/50 wt%) solution for electro-spinning was prepared by the following process. Concurrently, 15 g of PAN was dissolved in 100 mL of DMAc and 15 g of freeze-dried chitosan–methane sulfonic acid salt was dissolved in 100 mL of DMSO; then the two polymer solutions were blended together at ambient temperature for 4 h. An electro-spinner equipped with a high voltage DC generator (Chungpa EMT Co., Ltd., Seoul, Korea) and a syringe pump (Legato 200, KD Scientific, Holliston, MA, USA), was used. The voltage, flow rate and distance between the needle of the syringe and collector were 14 kV, 1 mL/h and 11 cm, respectively. Aluminum foil wrapped on a metal drum was used as the collector and the metal drum collector was rotating during collection. The coagulation and rinsing process for the electrospun nanofiber mat were same as the preparation of the films. The thickness of the nanofiber mat was approximately 200 μm. The nanofiber mats were applied to measure the antibacterial efficacy of the largely enhanced surface area of PAN–chitosan blend.

### 2.4. Instrumental analyses

The films and nanofiber mats of PAN and PAN/chitosan were coated with platinum under an argon purge prior to observations. The resulting samples were observed by scanning electron microscopy (SEM) (Hitachi S-4100, Tokyo, Japan) at a 15-kV accelerating voltage. To examine the cross-sections, the samples were frozen in liquid nitrogen for over 30 min and samples were then broken prior to observation. X-ray photoelectron spectroscopy (XPS) was used to confirm the presence of oxygen in chitosan. XPS measurements were conducted using a Quantera SXM (ULVAC-PHI, Ulvac, Tokyo, Japan). Monochromatic Al was used as an X-ray source. Beam size, beam power, electron source and pass energy were 100 μm, 100 W, 18 kV and 26 eV, respectively. The surface of the films and powder (chitosan only) was examined by Fourier transform infrared (FTIR) spectroscopy (Spectrum 100, PerkinElmer, Waltham, MA, USA) in attenuated total reflectance (ATR) mode. Germanium (Ge) ATR crystals were used as the internal reflection elements. The sample was held against one side of the Ge crystal. The background spectra were obtained with a Ge crystal and nitrogen gas in the absence of the film or powder. After drying at 105 °C for 2 h, the FTIR spectra of the samples were scanned from 700 to 4000 $cm^{-1}$ for 64 scans at a 2 $cm^{-1}$ resolution. The thermal behavior of the films and powder (chitosan only) was examined by differential scanning calorimetry (DSC) (DSC 2920, TA Instruments, New Castle, DE, USA) in the temperature range from 30 to 310 °C under nitrogen purge gas and at a heating rate of 20 °C/min. Dynamic mechanical analysis (DMA) was performed on 20 mm × 10 mm × 0.1 mm films using a dynamic mechanical analyzer (N535-0001, PerkinElmer, Waltham, MA, USA), which was used for the evaluation of dynamic moduli and mechanical damping ($\tan\delta$) under nitrogen purge gas in a temperature range of 30–200 °C at a frequency of 1 Hz and heating rate of 2 °C/min. The thermal character of the films and powder (chitosan only) was measured by thermogravimetric analysis (TGA) (Q500, TA Instruments, New Castle, DE, USA) at a scan rate of 30 °C/min from room temperature to 800 °C under a nitrogen purge.

### 2.5. Antibacterial test

The films and nanofiber mats were challenged with *Escherichia coli* KCTC 2441, *Pseudomonas aeruginosa* KCTC 1750, *Staphylococcus aureus* KCTC 1621, and *Micrococcus luteus* KCTC 10240 using the modified AATCC Test Method 100-2004. The used bacteria were incubated under optimal medium condition and temperature. A 1 mL of the culture fluid was then diluted with 9 mL of sterile distilled water followed by incubation using streak-plate method at 37 °C for 24 h. The total bacteria of *E. coli*, *P. aeruginosa*, *S. aureus*, and *M. luteus* were $6.80 \times 10^5$, $5.44 \times 10^5$, $5.20 \times 10^5$, and $7.32 \times 10^5$ cfu/mL, respectively. Bacterial suspensions (25 μL) prepared with pH 7 phosphate buffer were added to 1-$in^2$ sample swatches. A second swatch was sandwiched over the first to ensure contact between the suspension and the swatches. At contact times of 60 min, the samples were quenched with 5.0 mL of sterile 0.85% saline solution. The quenched samples were then diluted with pH 7 phosphate buffer and plated on Typticase soy agar. The plates were incubated at 37 °C for 24 h, and the number of bacteria was counted to determine the presence or absence of viable bacteria. The antibacterial test was replicated thrice.

## 3. Results and discussion

### 3.1. Morphology of PAN–chitosan blend

The morphology of the PAN–chitosan films and nanofibers was investigated by SEM. The surfaces of PAN and PAN–chitosan films

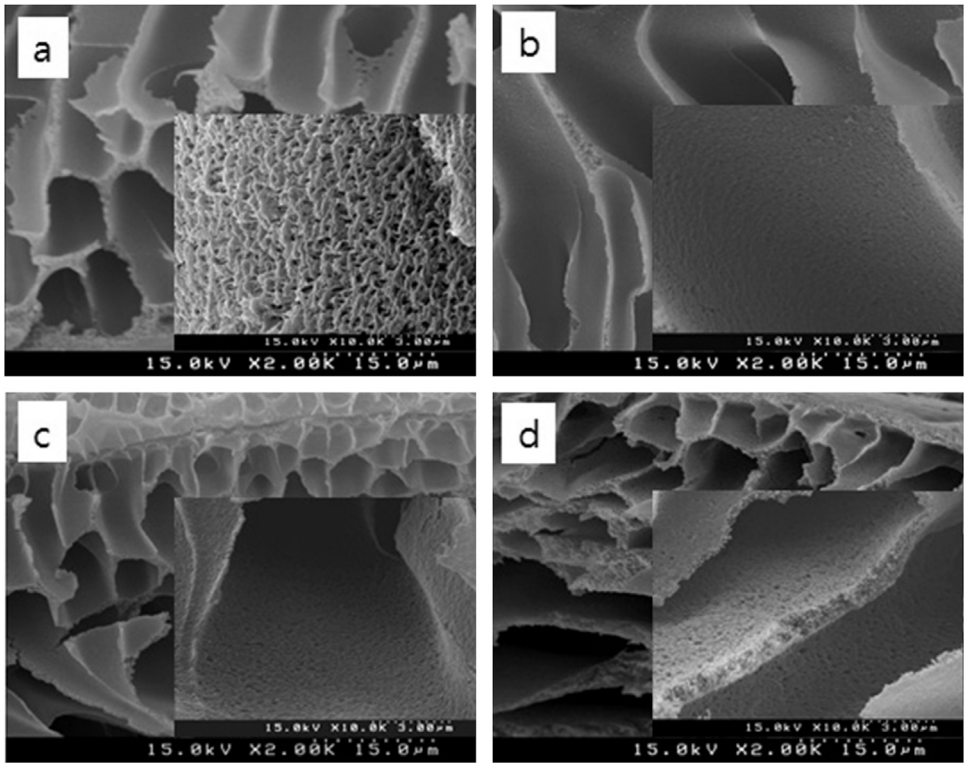


**Fig. 1.** Cross-sectional SEM images of PAN/chitosan blend films: (a) 100/0, (b) 85/15, (c) 75/25 and (d) 50/50 wt%.

were relatively flat and significant difference among the surface images was not found (no image in the paper). As comparison apparent properties of the films, the PAN film was not brittle; however, the PAN–chitosan films were relatively brittle and became more brittle with a higher ratio of chitosan in the blend. Notably 0/100 (PAN/chitosan, wt%) formed particles rather than film. This particle formation was presumably caused by the naturally brittle characteristic of chitosan (Nunthanid, Puttipipatkhachorn, Yamamoto, & Peck, 2001). The cross-sectional area surfaces of the blend films were explored to examine details of the dispersion of chitosan in PAN matrix (Fig. 1). The cross-sectional images of the PAN film and blend films exhibited a dense sponge-like structure that might be the resulting formation of different coagulation rate between the surface and inner position of the films (Kim & Lee, 2013). The images in Fig. 1 indicated that chitosan was blended uniformly throughout the PAN matrix until the content of chitosan was up to 50 wt%.

In general, nano-sized fibers possess increased surface area compared to regular fibers, and the dramatically increased surface area of the nano-sized fibers may provide a variety of novel properties and functions (Teo & Ramakrishna, 2006). Regarding suitability for electro-spinning, PAN/chitosan salt dissolved in DMSO did not form an electrospun mat, even though the electro-spinning factors had been adjusted. Thus, DMSO/DMAc co-solvent system (50/50, v/v) was used for the electro-spinning and the morphology of the nanofibers shown in Fig. 2. The diameters of PAN and PAN–chitosan electrospun nanofibers ranged from tens to thousands of nanometers. Unlike, the 85/15 wt% (PAN/chitosan) nanofibers, the PAN nanofibers had a relatively even diameter ranging in thousands of nanometers. During the electro-spinning using the DMSO/DMAc co-solvent, the electro-spinning conditions such as the voltage, flow rate and distance between the needle of the syringe and collector were also adjusted; however, the PAN–chitosan nanofiber mats other than the PAN nanofiber mat were barely formed. As explained above, chitosan was assumed to have a relatively brittle and low fiber-forming property. Thus, this relatively low fiber-forming property of chitosan was presumed to reduce the fiber-forming ability of the whole solution to spin the nanofiber

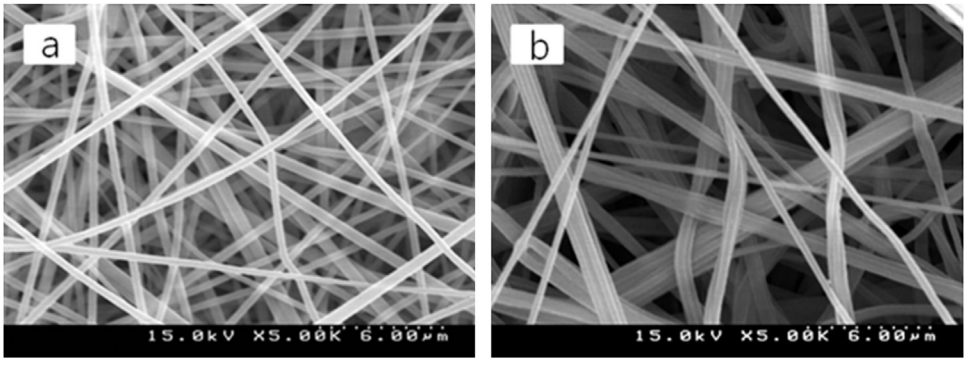


**Fig. 2.** SEM images of electrospun PAN/chitosan blends: (a) 100/0 and (b) 85/15 wt%.

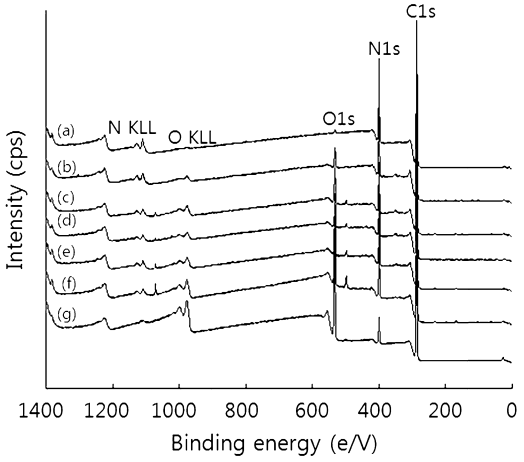


**Fig. 3.** XPS spectra of PAN/chitosan blend films: (a) 100/0, (b) 95/5, (c) 85/15, (d) 75/25, (e) 50/50, (f) 25/75, and (g) 0/100 (powder) wt%.

mats. Furthermore, additional electro-spinning technique such as atmospheric plasma may enhance the nanofiber mat forming properties of the blend (Shi, Vitchuli, Nowak, Caldwell, et al., 2011; Shi, Vitchuli, Nowak, Noar, et al., 2011; Vitchuli et al., 2012).

### 3.2. Characterization of PAN–chitosan blends

The surfaces of PAN, PAN–chitosan, and chitosan samples were analyzed by XPS; the spectra are shown in Fig. 3. Regarding chemical structure, chitosan contains oxygen atoms in its structure unlike PAN, and detection of oxygen would confirm the presence of chitosan in the blend. Oxygen peak (O1s) was observed at a binding energy of 531 eV in the chitosan spectrum (Fig. 3g) (Huang, Xu, Wan, Wang, & Wang, 2005). On the other hand, no definite oxygen peak was detected in the PAN spectrum. The peak at 531 eV was also found in the PAN–chitosan blends, and the intensity of the oxygen peak was enhanced with an increased ratio of chitosan. Thus, this oxygen peak in the blend presumably indicated that chitosan was incorporated in the blend.

The FTIR spectra of PAN–chitosan blends are shown in Fig. 4. The FTIR spectrum of PAN exhibited its distinctive absorption features at about 2937, 2243 and 1454 $cm^{-1}$, which were assigned to

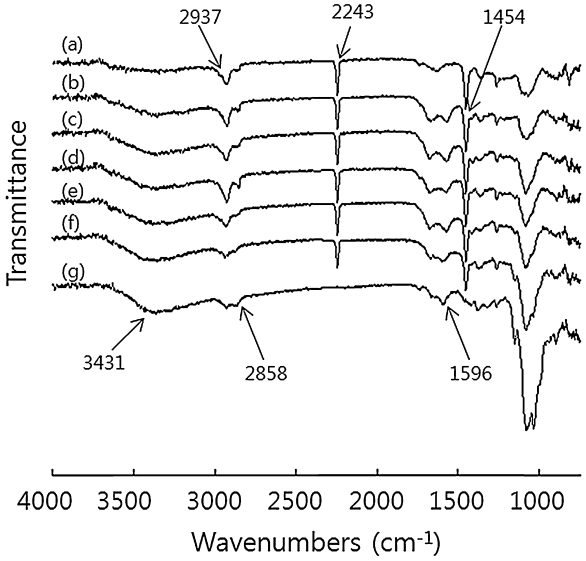


**Fig. 4.** FTIR spectra of PAN/chitosan blend films: (a) 100/0, (b) 95/5, (c) 85/15, (d) 75/25, (e) 50/50, (f) 25/75, and (g) 0/100 (powder) wt%.

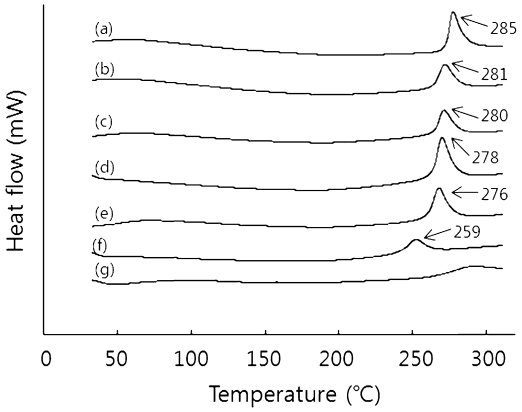


**Fig. 5.** DSC curves of PAN/chitosan blend films: (a) 100/0, (b) 95/5, (c) 85/15, (d) 75/25, (e) 50/50, (f) 25/75, and (g) 0/100 (powder) wt%.

C—H stretching, C≡N stretching, and $CH_2$ bending peaks, respectively (Rajendran, Babu, & Sivakumar, 2008). On the other hand, chitosan spectrum revealed a number of absorption bands at approximately 3431, 2858 and 1596 $cm^{-1}$, which were assigned to O—H stretching, C—H stretching and amine band, respectively (Jia et al., 2007). After PAN was blended with chitosan, the trenchant band at 2243 $cm^{-1}$ (C≡N) was observed in all the spectra of the blends. In addition to the C≡N stretching, other distinguishable peaks of PAN and chitosan such as bands at 3431 (O—H stretching, chitosan), 2937 (C—H stretching, PAN), 2858 (C—H stretching, chitosan), 1596 (amine band, chitosan), and 1454 ($CH_2$ bending, PAN) $cm^{-1}$ were found in the blends. These distinctive peaks in PAN–chitosan blends indicated that PAN and chitosan were undoubtedly blended. In this study, because the samples were dried at 105 °C for 2 h just before performing FTIR, the humidity (—OH) effect around 3200–3500 $cm^{-1}$ during the FTIR measurement would be limited. In the spectra of PAN/chitosan blends, the O—H stretching of chitosan was shown at 3431 $cm^{-1}$ which was found at same wavenumbers in the spectrum of chitosan. In addition, no FTIR band shift of $NH_2$ in chitosan or C≡N in PAN caused by molecular interaction was observed.

### 3.3. Thermal behavior and dynamic mechanical analysis

To analyze the thermal properties of PAN and chitosan, DSC analysis was performed and the results are shown in Fig. 5. Because of a cyclization reaction in PAN between a nitrile group and an adjacent nitrile group before melting, an exothermic transition of PAN caused by melting of crystal was not detected. An exothermic transition of the PAN film was observed at 285 °C (Fig. 5a) and this transition was presumed to indicate the cyclization reaction of PAN (Kim, 1996). The exothermic transition of PAN at 285 °C was shifted to lower temperature with an increased ratio of chitosan in the blend. In the case of PAN/chitosan (25/75, wt%), the exothermic transition was observed at 259 °C. The shift of exothermic transition of the PAN–chitosan blends indicated that incorporation of chitosan into PAN might influence the cyclization mechanism of PAN. On the other hand, chitosan showed an exothermic transition at 294 °C. This was considered to demonstrate oxidative decomposition of chitosan (Sreenivasan, 1996). In the blends, the oxidative decomposition of chitosan was not detected. On the other hand, molecular interaction could be examined using alteration of the glass transition temperature ($T_g$) of a polymer blend (Nam et al., 2001). This alteration of $T_g$ would vary due to molecular interaction in an amorphous region; however, the $T_g$ of PAN or chitosan was not detected when DSC was used (Fig. 5). We assumed that

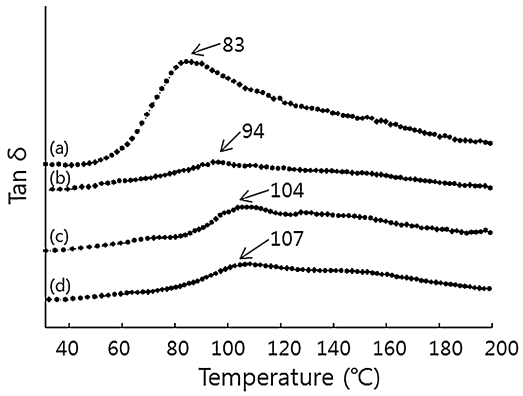


**Fig. 6.** Tan $\delta$ of PAN/chitosan blend films: (a) 100/0, (b) 95/5, (c) 85/15, and (d) 75/25 wt%.

the sensitivity of the DSC applied in this study was not sufficient to detect the $T_g$ of PAN or chitosan.

To measure $T_g$ of the blend films, DMA which was a different technique to confirm $T_g$ of polymers, was performed and the DMA results are shown in Fig. 6. The changing temperature of tan $\delta$ of PAN film was observed at 83 °C, which was defined as $T_g$ of PAN (Liu, Lin, Huang, Chen, & Yang, 2005). The $T_g$ of PAN was shifted to higher temperature with an enhanced portion of chitosan in the blend. For instance, the $T_g$ of 95/5 and 75/25 (PAN/Chitosan, wt%) were observed at 94 and 107 °C, respectively. Thus, the $T_g$ shift of PAN after blending with chitosan suggested that PAN and chitosan underwent a molecular interaction.

The TGA thermal curves are shown in Fig. 7. The pattern of TGA curve of the PAN film measured in inert atmosphere corresponded to a previous study (Ji et al., 2010). The yield residual mass of the PAN film at 800 °C was 35% and the first mass reduction began at around 280 °C associated with cyclization of the nitrile groups. The second degradation of the PAN film occurred at 300–450 °C might be related to the thermal degradation reaction of PAN (Korobeinyk, Whitby, & Mikhalovsky, 2012). In case of chitosan, two distinct mass losses at approximately 100 and 300 °C were considered as the loss of water and the thermal degradation of chitosan chain (Thanpitcha, Sirivat, Jamieson, & Rujiravanit (2006)), respectively. Regarding mass loss of the hybrid films, the blends containing 5–75 wt% of chitosan revealed three stages mass loss profiles. These were presumed to be caused by the evaporation of water, cyclization of the nitrile groups, and thermal degradation reaction. At 800 °C the yield

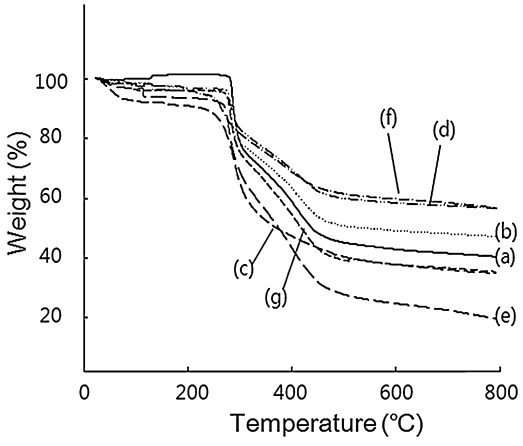


**Fig. 7.** TGA curves of PAN/chitosan blend films: (a) 100/0, (b) 95/5, (c) 85/15, (d) 75/25, (e) 50/50, (f) 25/75, and (g) 0/100 (powder) wt%.

**Table 1**
Antimicrobial efficacy of the double-face films and electrospun nanofibers after 60 min contact time.

| Samples (PAN/chitosan, wt%) | *E. coli*[a] | | *P. aeruginosa*[b] | | *S. aureus*[c] | | *M. luteus*[d] | |
|---|---|---|---|---|---|---|---|---|
| | Bacterial no. (cfu/mL)[e] | Log reduction | Bacterial no. (cfu/mL)[e] | Log reduction | Bacterial no. (cfu/mL)[e] | Log reduction | Bacterial no. (cfu/mL)[e] | Log reduction |
| Film (100/0) | $5.21 \pm 0.77 \times 10^5$ | 0.12 | $4.04 \pm 0.46 \times 10^5$ | 0.13 | $3.86 \pm 0.24 \times 10^5$ | 0.13 | $5.81 \pm 0.52 \times 10^5$ | 0.10 |
| Film (85/15) | $1.15 \pm 0.51 \times 10^5$ | 0.77 | $2.97 \pm 0.30 \times 10^5$ | 0.26 | $5.12 \pm 0.38 \times 10^4$ | 1.01 | $5.57 \pm 0.29 \times 10^4$ | 1.12 |
| Nanofiber (100/0) | $5.05 \pm 0.33 \times 10^5$ | 0.13 | $4.19 \pm 0.23 \times 10^5$ | 0.11 | $4.20 \pm 0.54 \times 10^5$ | 0.09 | $5.38 \pm 0.31 \times 10^5$ | 0.13 |
| Nanofiber (85/15) | 0 | 5.83 | $6.89 \pm 0.81 \times 10^4$ | 0.90 | 0 | 5.71 | 0 | 5.86 |

[a] Total bacteria: $6.80 \times 10^5$ cfu/mL
[b] Total bacteria: $5.44 \times 10^5$ cfu/mL
[c] Total bacteria: $5.20 \times 10^5$ cfu/mL
[d] Total bacteria: $7.32 \times 10^5$ cfu/mL
[e] Bacterial No. data are expressed as mean ± standard deviation of a triplicate analysis.

residual mass of the hybrid films exhibited ranged from 37% to 58%.

### 3.4. Antibacterial efficacy

As outlined in the introduction, the major purpose of this study was to produce and confirm an antibacterial PAN–chitosan nanofibers. The antibacterial properties of PAN–chitosan double-face films and electrospun nanofibers were measured and the results are shown in Table 1. The 85/15 (PAN/chitosan, wt%) film revealed 0.2–1-log reduction against bacteria within 60 min contact time. On the other hand, the 85/15 (PAN/chitosan, wt%) nanofiber mat indicated 5-log reduction against *E. coli*, *S. aureus*, and *M. luteus* within 60 min contact time. On the other hand, the 85/15 (PAN/chitosan, wt%) nanofiber mat showed 0.9-log reduction against *P. aeruginosa*. As shown in the ratio between PAN and chitosan (85/15, PAN/chitosan, wt%), the ratio of the film and nanofiber mat were identical; however, the antibacterial efficacy was varied. This demonstrated that the nanofiber mat possessed improved antibacterial effectiveness with the equal blend ratio. The nanofiber mat was consisted of nano-sized fibers and the surface area of the nanofiber mat was increased dramatically in comparison to the film which had flat surface. The surface area of nanofiber mat relatively increased, was presumed to indicate that the amount of cationic amine ($-NH_3^+$) of chitosan in the surface was also increased. Therefore, the improved antibacterial efficacy might be obtained by the cationic amine in the enlarged surface of the nanofibers.

## 4. Conclusion

After forming nanofibers, the PAN–chitosan electrospun nanofibers showed significantly enhanced antibacterial properties. The nanofibers possessed more chitosan which inactivate bacteria on the surface than the surface of double-face films. Antibacterial efficacy was dependent on the surface area of the PAN–chitosan blend. The large surface area, water insolubility, and antibacterial properties of the PAN–chitosan electrospun nanofibers are well suited to applications of PAN and chitosan in antibacterial fibers and membranes. In our future research, an additional technique such as atmospheric plasma to improve nanofiber forming properties during electro-spinning of PAN–chitosan blend will be explored.

## Acknowledgements

The authors wish to thank Kwangho Choi of the Department of Applied Microbiology and Biotechnology, Yeungnam University, for the preparation of the antibacterial test. The authors are also grateful to Jimin Lee for her helpful discussion and for preparing the samples.

## References

Chaudhari, L. B., & Murthy, Z. V. P. (2013). Preparation, characterization, and performance of sulfated chitosan/polyacrylonitrile composite nanofiltration membranes. *Journal of Dispersion Science and Technology*, *34*, 389–399.

Dastjerdi, R., & Montazer, M. (2010). A review on the application of inorganic nano-structured materials in the modification of textiles: Focus on anti-microbial properties. *Colloids and Surfaces B: Biointerfaces*, *79*, 5–18.

Gao, Y., & Cranston, R. (2008). Recent advances in antimicrobial treatments of textiles. *Textile Research Journal*, *78*, 60–72.

Huang, X., Xu, Z., Wan, L., Wang, Z., & Wang, J. (2005). Surface modification of polyacrylonitrile-based membranes by chemical reactions to generate phospholipid moieties. *Langmuir*, *21*, 2941–2947.

Jeong, S. H., Hwang, Y. H., & Yi, S. C. (2005). Antibacterial properties of padded PP/PE nonwovens incorporating nano-sized silver colloids. *Journal of Materials Science*, *40*, 5413–5418.

Ji, L., Yao, Y., Toprakci, O., Lin, Z., Liang, Y., Shi, Q., et al. (2010). Fabrication of carbon nanofiber-driven electrodes from electrospun polyacrylonitrile/polypyrrole bicomponents for high-performance rechargeable lithium-ion batteries. *Journal of Power Sources*, *195*, 2050–2056.

Jia, Y., Gong, J., Gu, X., Kim, H., Dong, J., & Shen, X. (2007). Fabrication and characterization of poly(vinyl alcohol)/chitosan blend nanofibers produced by electrospinning method. *Carbohydrate Polymers*, *67*, 403–409.

Kim, H. S. (1996). Thermal behavior of polyacrylonitrile and poly(vinylpyrrolidone-graft-acrylonitrile) blend. *Journal of Polymer Science Part B: Polymer Physics*, *34*, 1181–1187.

Kim, S., & Lee, J. (2013). Antimicrobial polyacrylonitrile/*m*-aramid hybrid composite. *Industrial Engineering Chemistry Research*, *52*, 10297–10304.

Kim, Y. H., & Sun, G. (2001). Durable antimicrobial finishing of nylon fabrics with acid dyes and a quaternary ammonium salt. *Textile Research Journal*, *71*, 318–323.

Kim, S., Kim, J., Huang, T. S., Whang, H. S., & Lee, J. (2009). Antimicrobial polyethylene terephthalate (PET) treated with an aromatic *N*-halamine precursor, *m*-aramid. *Journal of Applied Polymer Science*, *114*, 3835–3840.

Korobeinyk, A. V., Whitby, R. L. D., & Mikhalovsky, S. V. (2012). High temperature oxidative resistance of polyacrylonitrile-methylmethacrylate copolymer powder converting to a carbonized monolith. *European Polymer Journal*, *48*, 97–104.

Lee, J., & Whang, H. S. (2011). Poly(vinyl alcohol) blend film with *m*-aramid as an *N*-halamine precursor for antimicrobial activity. *Journal of Applied Polymer Science*, *122*, 2345–2350.

Liu, C., & Bai, R. (2006). Adsorptive removal of copper ions with highly porous chitosan/cellulose acetate blend hollow fiber membranes. *Journal of Membrane Science*, *284*, 313–322.

Liu, T., Lin, W., Huang, L., Chen, S., & Yang, M. (2005). Surface characteristics and hemocompatibility of PAN/PVDF blend membranes. *Polymer for Advanced Technologies*, *16*, 413–419.

Muzzarelli, R. A. A. (1993). Biochemical significance of exogenous chitins and chitosans in animals and patients. *Carbohydrate Polymers*, *20*, 7–16.

Muzzarelli, R. A. A., Tarsi, R., Filippini, O., Giovanetti, E., Biagini, G., & Varaldo, P. E. (1990). Antimicrobial properties of *N*-carboxybutyl chitosan. *Antimicrobial Agents and Chemotherapy*, *34*, 2019–2023.

Muzzarelli, R. A. A., Boudrant, J., Meyer, D., Manno, N., DeMarchis, M., & Paoletti, M. G. (2012). A tribute to Henri Braconnot, precursor of the carbohydrate polymers science, on the chitin bicentennial. *Carbohydrate Polymers*, *87*, 995–1012.

Nakashima, T., Sakagami, Y., & Matsuo, M. (2001). Antibacterial efficacy of cotton fabrics chemically modified by metal salts. *Biocontrol Science*, *6*, 9–15.

Nam, C., Kim, Y., & Ko, S. (1999). Modification of polyacrylonitrile (PAN) fiber by blending with *N*-(2-hydroxy)propyl-3-trimethyl-ammonium chitosan chloride. *Journal of Applied Polymer Science*, *74*, 2258–2265.

Nam, C., Kim, Y., & Ko, S. (2001). Blend fibers of polyacrylonitrile and water-soluble chitosan derivative prepared from sodium thiocyanate solution. *Journal of Applied Polymer Science*, *82*, 1620–1629.

Nataraj, S. K., Yang, K. S., & Aminabhavi, T. M. (2012). Polyacrylonitrile-based nanofibers: A state-of-the-art review. *Progress in Polymer Science*, *37*, 487–513.

Nunthanid, J., Puttipipatkhachorn, S., Yamamoto, K., & Peck, G. E. (2001). Physical properties and molecular behavior of chitosan films. *Drug Development and Industrial Pharmacy*, *27*, 143–157.

Rajendran, S., Babu, R. S., & Sivakumar, P. (2008). Ionic conduction in plasticized PVC/PAN blend polymer electrolytes. *Ionics*, *14*, 149–155.

Ren, X., Kocer, H. B., Kou, L., Worley, S. D., Broughton, R. M., Tzou, Y. M., et al. (2008). Antimicrobial polyester. *Journal of Applied Polymer Science*, *109*, 2756–2761.

Ren, X., Akdag, A., Zhu, C., Kou, L., Worley, S. D., & Huang, T. S. (2009). Electrospun polyacrylonitrile nanofibrous biomaterials. *Journal of Biomedical Materials Research Part A*, *91A*, 385–390.

Sashiwa, H., Shigemasa, Y., & Roy, R. (2000). Dissolution of chitosan in dimethyl sulfoxide by salt formation. *Chemistry Letters*, *29*, 596–597.

Shi, Q., Vitchuli, N., Nowak, J., Caldwell, J. M., Breidt, F., Bourham, M., et al. (2011). Durable antibacterial Ag/polyacrylonitrile (Ag/PAN) hybrid nanofibers prepared by atmospheric plasma treatment and electrospinning. *European Polymer Journal*, *47*, 1402–1409.

Shi, Q., Vitchuli, N., Nowak, J., Noar, J., Caldwell, J. M., Breidt, F., et al. (2011). One-step synthesis of silver nanoparticle-filled nylon 6 nanofibers and their antibacterial properties. *Journal of Materials Chemistry*, *21*, 10330–10335.

Sreenivasan, K. (1996). Thermal stability studies of some chitosan–metal ion complexes using differential scanning calorimetry. *Polymer Degradation and Stability*, *52*, 85–87.

Srinivasa, P. C., Ramesh, M. N., Kumar, K. R., & Tharanathan, R. N. (2003). Properties and sorption studies of chitosan–polyvinyl alcohol blend films. *Carbohydrate Polymers*, *53*, 431–438.

Sudarshan, N. R., Hoover, D. G., & Knorr, D. (1992). Antibacterial action of chitosan. *Food Biotechnology*, *6*, 257–272.

Takahashi, T., Shoji, Y., Inoue, O., Miyamoto, Y., & Tokuda, K. (2004). Antibacterial properties of rayon fibers containing titanium oxide photocatalyst. *Biocontrol Science*, *9*, 51–60.

Teo, W. E., & Ramakrishna, S. (2006). A review on electrospinning design and nanofibre assemblies. *Nanotechnology*, *17*, R89–R106.

Thanpitcha, T., Sirivat, A., Jamieson, A. M., & Rujiravanit, R. (2006). Preparation and characterization of polyaniline/chitosan blend film. *Carbohydrate Polymers*, *64*, 560–568.

Torres-Giner, S., Ocio, M. J., & Lagaron, J. M. (2008). Development of active antimicrobial fiber-based chitosan polysaccharide nanostructures using electrospinning. *Engineering in Life Sciences*, *8*, 303–314.

Vitchuli, N., Shi, Q., Nowak, J., Nawalakhe, R., Sieber, M., Bourham, M., et al. (2012). Plasma-electrospinning hybrid process and plasma pretreatment to improve adhesive properties of nanofibers on fabric surface. *Plasma Chemistry Plasma Processing*, *32*, 275–291.

Wan, Y., Wu, H., Yu, A., & Wen, D. (2006). Biodegradable polylactide/chitosan blend membranes. *Biomacromolecules*, *7*, 1362–1372.

Zhang, H., Li, S., White, C. J. B., Ning, X., Nie, H., & Zhu, L. (2009). Studies on electrospun nylon-6/chitosan complex nanofiber interactions. *Electrochimica Acta*, *54*, 5739–5745.

Zhu, P., & Sun, G. (2004). Antimicrobial finishing of wool fabrics using quaternary ammonium salts. *Journal of Applied Polymer Science*, *93*, 1037–1041.